Error Statistics for Average Power Measurements in Wireless Communication Systems

Shuangqing Wei, *Student Member, IEEE,* and Dennis L. Goeckel, *Member, IEEE*

***Abstract*—The measurement of the average received power is essential for power control and dynamic channel allocation in wireless communication systems. However, due to the effects of multipath fading and additive noise inherent to the wireless channel, there can be significant errors in such measurements. In this paper, the error statistics for average power measurements are considered; in particular, the probability distribution of the value of the average received power at the time of interest conditioned on an outdated measurement is obtained. The resulting expression should have high utility in the analysis of wireless communication systems. However, in this paper, the design of power control algorithms that minimize the average transmitted power required to achieve a desired outage probability for the link is considered. A number of novel power control algorithms based on various models for the error in the average power measurement are derived. Numerical results indicate that power control algorithms based on the accurate expression derived in this paper can demonstrate significant gains over those based on previous approximate models.**

***Index Terms*—Average power measurement, dynamic channel allocation, fading channels, power control.**

I. Introduction

In WIRELESS communication systems, the transmission environment can vary greatly as conditions evolve over time. This is due not only to the variation in the path loss caused by changes in the distance between the transmitter and the receiver, but also to shadowing and multipath fading. Thus, adaptation of the transmitter parameters to the current transmission environment is imperative to avoid the losses in system performance that result from prescribing a system with constant parameters that are set such that the system performs acceptably under the worst possible operating conditions. Although recent work in adaptive signaling has considered adaptation to fast multipath fading [1]–[3], historically, adaptation has been done in response to characteristics of the environment that are constant over a relatively long period of time, such as the local average power, where the averaging is over the multipath fading.

Paper approved by F. Santucci, the Editor for Wireless System Performance of the IEEE Communications Society. Manuscript received September 10, 2000; revised July 17, 2001 and December 14, 2001. This work was supported in part by the National Science Foundation under Grant NCR-9714597 and CAREER Award CCR-9875482. This paper was presented in part at the Thirty-Third Asilomar Conference on Signals, Systems, and Computers, Pacific Grove, CA, October 1999, and at the International Communications Conference, Helsinki, Finland, June 2001.

The authors are with the Electrical and Computer Engineering Department, University of Massachusetts, Amherst, MA 01003-5110 USA (e-mail: goeckel@ecs.umass.edu).

Publisher Item Identifier 10.1109/TCOMM.2002.802569.

Different adaptation schemes that require measurements of the local average power, such as data-rate adaptation, power control, and handoff algorithms, have been proposed to increase spectral efficiency, power efficiency, and system capacity. In the second- and third-generation packet data standards, data-rate adaptations generally considered are slow rate adaptations. The data rate is adapted in response to shadowing and path loss over the coverage area. In code-division multiple-access (CDMA) systems, pilot strength measurements are used to estimate the signal-to-interference-plus-noise ratio (SINR) at the receiver. By making use of such information about the channel quality, rate adaptation is achieved through a combination of variable spreading, coding, and code aggregation [4]. Handoffs in cellular communication, whereby a mobile subscriber communicating with one base station is switched to another base station during a call [5], [6], also employ average power measurements. In many systems, especially microcellular systems, signal strength may be the only reliable measurement that can be used to make such handoff decisions [6]. In CDMA systems, to effectively implement soft handover as described in [7], the controlling base station (BS) is selected from within the active set according to the slow shadowing measurements of the channel between the mobile station (MS) and each BS in that set. Finally, the use of transmitter power control has been proposed to control cochannel interference. The main idea is to adjust the transmitter power, based on the measurements of the slow channel variation such that the large scale shadowing of the channel can be compensated [8], [9].

It is obvious that those adaptation schemes discussed in the previous paragraph all require knowledge of the local power averaged over the multipath fading. However, the effects of the multiplicative fading and additive noise can lead to significant errors in the measurements of the average received signal power. In [10], it was argued that the distribution of the estimation error in the average power under combined Rayleigh fading and shadowing follows a log-normal distribution. Because of the wide applicability of such a model, it has been referenced often in the short time since [10] appeared. In particular, [11] considers the effects of imperfect average power measurements on adaptive M-ary quadrature amplitude modulation (MQAM), where the transmit power and data rate are varied based on the channel gain. In [5], the model of [10] is used to understand BS selections. In particular, in cellular CDMA networks, the selection of the controlling BS is made based on the local mean estimation from a sequence of power level measurements that the MS takes on the pilot channels broadcast by the various BSs. From the estimation error model in [10], the analysis in [5] is able to provide a characterization of the membership switching, in terms of how

frequently this switching may be required and to what extent fast fading contributes to a nonoptimal BS selection. Finally, under the same measurement error statistical model, the effect of the power control error on the system capacity of a CDMA mobile satellite link is analyzed in [9].

The statistical model for the measurement error can be employed not only in system performance analyses as described above, but also in system design. In this paper, such a model will be employed to design power control algorithms. In power control problems, the path gains and log-normal shadowing of the users are usually assumed to be perfectly known by the receivers (see [12] and references therein). However, in practical implementations, they are measured at the receiver end, which results in measurement uncertainty. The idea of stochastic power control was proposed in [13]. In [13], variation in the measurements of the average received power is caused by randomness in both the data transmitted by the users and the additive noise; assuming that there is a feasible solution to the power control problem, algorithms are presented which converge in the mean-square sense to the optimal power control vector. In this paper, the randomness is due to the multipath fading and additive noise. Instead of attempting to prescribe an algorithm which evolves over time to the optimal power solution, such that all user signal-to-interference ratio (SIR) requirements are met, a small outage probability is allowed for each user. This allows the statistical dependence of the average received SIR on the measurement of the average received SIR to be exploited to prescribe a power control algorithm, such that the outage probability of each user is met with the minimum required transmit power. An alternative method to deal with the measurement uncertainty is to increase the signaling margin of the system to account for the worst-case level of uncertainty; however, in cases where there is a well-accepted statistical model for the measurement error, it may be feasible to adapt the system parameters in such a way that it accounts for this measurement uncertainty directly.

For a single-user system, a closed form power control rule is found in our previous work [14] under the model for measurement error developed in [10]; the resulting rule suggests a moderate gain over systems which employ traditional power control functions with an energy margin to compensate for measurement uncertainty. However, in [10], the additive noise is not taken into account, and the successive samples of the received signal power are assumed to be uncorrelated when developing the log-normal form of the measurement error model; these assumptions result in a Gamma distribution for the measurement. (Note that the correlation of the samples *is* included in [10] when deriving the *parameters* of the log-normal distribution of the measurement error.) The goal of this paper is to study the conditional distribution function of the actual slow shadowing given the measurement, while taking into account both the impact of additive noise and the correlated nature of the Rayleigh fading. Furthermore, the optimum power control rule will be developed under the derived measurement error model for a single-user system. Thus, there are two contributions of this paper: 1) an accurate model for the error in average power measurements, which can be used for system design and analysis, or to verify other approximate models, and 2) a novel approach to power control under measurement uncertainty, which includes the derivation of a number of novel power control algorithms.

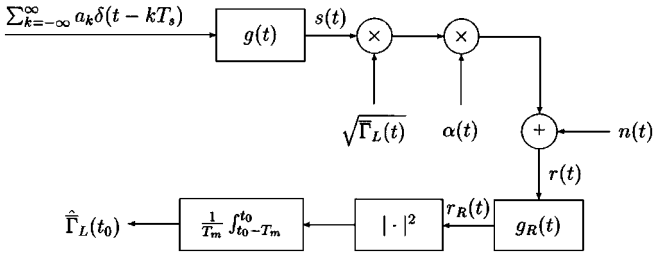

Fig. 1. System and measurement model.

The remainder of this paper is organized as follows. In Section II, the system and measurement models are outlined. In Section III, the desired conditional distribution is derived analytically by employing Toeplitz matrix theory, and the result is verified numerically. An accurate approximation to the desired conditional distribution function is developed. Finally, in Section IV, optimal power control rules are developed under different measurement error statistical models, and their performance is compared. Section V presents the conclusions.

II. Model and Characterization

A. System Model

In this paper, only the single-user case is considered. A frequency nonselective, slowly fading channel as shown in Fig. 1 will be assumed; thus, the transmitted signal is affected by a multiplicative process, which may be regarded as constant over the support of a given symbol pulse [15]. The complex baseband representation of the received signal $r(t)$ is given by

$$r(t) = \sqrt{\overline{\Gamma}_L(t)}\alpha(t)s(t) + n(t) \tag{1}$$

where $\overline{\Gamma}_L(t)$ is the real-valued factor caused by path loss and the shadowing due to objects between the transmitter and receiver [16], $\alpha(t)$ is the complex-valued fast-fading factor due to the multipath short-term fading [16], and $n(t)$ is the additive white complex-valued Gaussian noise, which is independent of $\overline{\Gamma}_L(t)$ and $\alpha(t)$. The signal $s(t) = \sum_{k=-\infty}^{\infty} a_k g(t - kT_s)$ is the low-pass representation of the transmitted signal, where a_k is the kth transmitted symbol, and $g(t)$ is the unit-energy baseband pulse shape, which is assumed for simplicity to have the band-limited frequency response characteristic

$$G(f) = \begin{cases} \sqrt{T_s}, & |f| \le \frac{1}{2T_s} \\ 0, & \text{otherwise} \end{cases}$$

where $1/T_s$ is the symbol rate. It will be assumed that a pilot channel is being used for signal strength measurement; thus, let $a_k = \sqrt{E_T}, \forall\, k$, where E_T is the average transmitted energy per symbol. Assuming the Gaussian wide-sense stationary uncorrelated scattering (GWSSUS) model [18]

$$\alpha(t) = \alpha_I(t) + j\alpha_Q(t)$$
$$n(t) = n_I(t) + jn_Q(t)$$

where $\alpha_I(t)$ and $\alpha_Q(t)$ are independent Gaussian random processes, each with zero mean and autocorrelation function [16], [17]

$$E[\alpha_I(t)\alpha_I(t+\tau)] = E[\alpha_Q(t)\alpha_Q(t+\tau)] = \frac{1}{2}J_0(2\pi f_d\tau) \quad (2)$$

where $f_d = \nu/\lambda$ is the maximum Doppler shift, ν is the mobile velocity, and λ is the wavelength of the carrier signal. The processes $n_I(t)$ and $n_Q(t)$ are independent white Gaussian noise processes, each with zero mean and two-sided power spectral density N_0.

It is generally assumed that the marginal distributions of the shadowing process are log-normal [16]; that is, for a fixed t, $\ln\overline{\Gamma}_L(t)$ is normally distributed with mean μ and standard deviation σ_Y, both in nepers (Np), where μ corresponds to the path loss. Since the shadowing is generally estimated over a time interval which is only on the order of several times the inverse of the channel bandwidth, the path loss is assumed to be constant over the measurement interval [10] and it is available to the receiver. Furthermore, $\ln\overline{\Gamma}_L(t)$ can generally be treated as a Gaussian random process, with mean μ and autocovariance function given by [19]

$$A_{\ln\overline{\Gamma}_L}(\tau) = \sigma_Y^2 \exp\left(\frac{-\nu|\tau|}{X_c}\right) \quad (3)$$

where X_c is the effective correlation distance of the shadowing. It should be noted that the form of the autocorrelation functions for the multipath fading and shadowing in (2) and (3), respectively, will impact the numerical results when used for analysis purposes, although the same derivation method can easily be applied for other autocorrelation functions. Issues to robustness across uncertainties in these functions is important, particularly for design [3], and will be the subject of future work.

The received signal $r(t)$ is passed through a noise-limiting lowpass filter matched to the transmitted pulse to yield

$$r_R(t) = r(t) * g_R(t)$$

where $G_R(f) = G^*(f)$, and $x(t) * y(t)$ is the convolution of $x(t)$ and $y(t)$.

B. Measurement Model

1) Continuous-Time Model: One practical method of measuring the average received power is to employ an integrate-and-dump (I&D) filter, as shown in Fig. 1 [10], [20]. The average received power measurement is then given by (4) shown at the bottom of the page, where $\hat{\overline{\Gamma}}_L(t_0)$ is the measured value of $\overline{\Gamma}_L(t_0)$, T_m is the duration of the measurement window, and $n_R(t) = n_{R,I}(t) + jn_{R,Q}(t)$ is a complex-valued zero-mean Gaussian noise process, whose autocorrelation function is given by

$$\begin{aligned} E[n_{R,I}(t)n_{R,I}(t+\tau)] &= E[n_{R,Q}(t)n_{R,Q}(t+\tau)] \\ &= N_0\frac{\sin\left(\frac{\pi\tau}{T_s}\right)}{\frac{\pi\tau}{T_s}} \end{aligned} \quad (5)$$

where N_0 here has included the factor of path loss and the transmitted power after normalization by them (i.e., reciprocal of the ratio of received signal power to noise power). As in [21], it will be assumed that $\overline{\Gamma}_L(t)$ can be modeled as constant in this window; hence, it will be assumed that $\overline{\Gamma}_L(t) = C^2$, for $t \in [t_0 - T_m, t_0]$, and thus the measurement error is due to the variation in the short-term fading and noise.

2) Discrete-Time Model: Measurement of the average received power is often done in the discrete domain [9], [22]. Let $Z_n^{(N)} = (1/\sqrt{N})r_R(t_0 - T_m + nT_s)$, $n = 0, \ldots, N-1$, be the nth normalized sample of the filtered received signal, where the sampling has been done at the Nyquist rate, and $N = \lceil T_m/T_s \rceil$ is the number of sample points corresponding to a window of duration T_m. As stated in [22], for the linear power measurement method considered here, the performance improvement of the optimal local mean signal level estimator (optimum minimum variance unbiased estimator) for the Rayleigh fading environment over the traditional sample average estimator is minimal; hence, in this work, the traditional sample average estimator is considered. Thus, the estimator of the slow shadowing in the discrete-time case is given by

$$\hat{\overline{\Gamma}}_L^{(N)} = \sum_{n=0}^{N-1} |Z_n^{(N)}|^2. \quad (6)$$

Let $\mathbf{Z}^{(N)} = \left[Z_0^{(N)}, \ldots, Z_{N-1}^{(N)}\right]^T$, $\mathbf{X}^{(N)} = \left[X_0^{(N)}, \ldots, X_{N-1}^{(N)}\right]^T$, and $\mathbf{Y}^{(N)} = \left[Y_0^{(N)}, \ldots, Y_{N-1}^{(N)}\right]^T$, where $(\,)^T$ is the transpose of a vector. Note $\mathbf{Z}^{(N)} = \mathbf{X}^{(N)} + j\mathbf{Y}^{(N)}$, where $\mathbf{X}^{(N)}$ and $\mathbf{Y}^{(N)}$ are independent Gaussian random vectors with

$$\begin{aligned} E\left[X_n^{(N)}\right] &= E\left[Y_n^{(N)}\right] = 0 \\ E\left[X_n^{(N)}X_m^{(N)}\right] &= E\left[Y_n^{(N)}Y_m^{(N)}\right] \\ &= \frac{1}{2N}C^2J_0(2\pi f_d(n-m)T_s) \\ &\quad + \frac{N_0}{N}\delta(n-m) \\ n, m &= 0, \ldots, N-1 \end{aligned} \quad (7)$$

where $\delta(\cdot)$ is the Kronecker Delta function. The discrete-time model also will provide a reasonable approximation of the con-

$$\hat{\overline{\Gamma}}_L(t_0) = \frac{1}{T_m}\int_{t_0-T_m}^{t_0} |r_R(v)|^2 dv = \frac{1}{T_m}\int_{t_0-T_m}^{t_0} \left|\sqrt{\overline{\Gamma}_L(v)}\alpha(v)\sum_{k=-\infty}^{\infty} g(v - kT_s) * g_R(v) + n_R(v)\right|^2 dv \quad (4)$$

tinuous-time model; thus, the discrete-time model is considered for the rest of this paper.

C. Conditional Distribution

In any practical application, there will be delay between the time the shadowing estimate is made and the time the corresponding estimate is employed for system adjustments. Hence, it is of interest to find the conditional density function $f_{\overline{\Gamma}_L(t_0+\tau)|\hat{\overline{\Gamma}}_L(t_0)}(\cdot|\cdot)$ of the shadowing at the time of interest $t_0+\tau$, given the measured value of the shadowing at an earlier time t_0

$$\begin{aligned} f_{\overline{\Gamma}_L(t_0+\tau)|\hat{\overline{\Gamma}}_L(t_0)}(z|x) &= \int f_{(\overline{\Gamma}_L(t_0+\tau),\overline{\Gamma}_L(t_0))|\hat{\overline{\Gamma}}_L(t_0)}(z,y|x)\,dy \\ &= \int f_{\overline{\Gamma}_L(t_0)|\hat{\overline{\Gamma}}_L(t_0)}(y|x) \\ &\quad \times f_{\overline{\Gamma}_L(t_0+\tau)|(\hat{\overline{\Gamma}}_L(t_0),\overline{\Gamma}_L(t_0))} \\ &\quad \times (z|x,y)dy. \end{aligned} \tag{8}$$

According to the measurement model, $\overline{\Gamma}_L(t_0+\tau)$ is conditionally independent of $\hat{\overline{\Gamma}}_L(t_0)$, when given $\overline{\Gamma}_L(t_0)$. Thus, $f_{\overline{\Gamma}_L(t_0+\tau)|(\hat{\overline{\Gamma}}_L(t_0),\overline{\Gamma}_L(t_0))}(z|x,y) = f_{\overline{\Gamma}_L(t_0+\tau)|\overline{\Gamma}_L(t_0)}(z|y)$, and it follows that

$$\begin{aligned} f_{\overline{\Gamma}_L(t_0+\tau)|\hat{\overline{\Gamma}}_L(t_0)}(z|x) = \frac{1}{f_{\hat{\overline{\Gamma}}_L(t_0)}(x)} \times \int f_{\hat{\overline{\Gamma}}_L(t_0)|\overline{\Gamma}_L(t_0)}(x|y) \\ f_{(\overline{\Gamma}_L(t_0),\overline{\Gamma}_L(t_0+\tau))}(y,z)\,dy. \end{aligned} \tag{9}$$

Since $\ln\overline{\Gamma}_L(t)$ is a Gaussian random process whose autocorrelation function is known, the difficulty lies in finding $f_{\hat{\overline{\Gamma}}_L(t_0)|\overline{\Gamma}_L(t_0)}(x|y)$.

III. Asymptotic Conditional Density Function

In order to find $f_{\hat{\overline{\Gamma}}_L(t_0)|\overline{\Gamma}_L(t_0)}(x|y=C^2)$, it is necessary to study the statistics of the output of the measurement filter. For any reasonably reliable estimator of $\overline{\Gamma}_L(t)$, $N=\lceil T_m/T_s\rceil$ is large. Hence, the asymptotic (large N) statistics of the output of the sample average estimator are studied in this section.

A. Matrix Transformation

The measurement $\hat{\overline{\Gamma}}_L^{(N)}$ in (6) is a quadratic form of the vector $\mathbf{Z}^{(N)}$. Let $\mathbf{Z}^{(N)H}$ be the complex conjugate transpose of $\mathbf{Z}^{(N)}$. Then

$$\begin{aligned} \hat{\overline{\Gamma}}_L^{(N)} &= \mathbf{Z}^{(N)H}\cdot\mathbf{Z}^{(N)} \\ &= \mathbf{X}^{(N)^T}\cdot\mathbf{X}^{(N)} + \mathbf{Y}^{(N)^T}\cdot\mathbf{Y}^{(N)}. \end{aligned} \tag{10}$$

From (7), the autocorrelation matrix of the vectors $\mathbf{X}^{(N)}$ and $\mathbf{Y}^{(N)}$ are $R_{\mathbf{X}^{(N)}} = E\left[\mathbf{X}^{(N)}\mathbf{X}^{(N)^T}\right]$ and $R_{\mathbf{Y}^{(N)}} = E\left[\mathbf{Y}^{(N)}\mathbf{Y}^{(N)^T}\right]$, respectively, where

$$\begin{aligned} (R_{\mathbf{X}^{(N)}})_{i,j} &= \frac{1}{2N}C^2 J_0[2\pi f_d(i-j)T_s] \\ &\quad + \frac{N_0}{N}\delta(i-j), \\ i,j &= 0,\ldots,N-1. \end{aligned} \tag{11}$$

The matrix $R_{\mathbf{X}^{(N)}}$ is symmetric, Toeplitz, and nonnegative definite. Thus, $\left\{\lambda_0^{(N)},\ldots,\lambda_{N-1}^{(N)}\right\}$, the eigenvalues of $R_{\mathbf{X}^{(N)}}$, are real and greater than or equal to zero. Thus, there exists an orthogonal matrix $P^{(N)}$ [23] such that for $\tilde{\mathbf{X}}^{(N)} = P^{(N)^T}\mathbf{X}^{(N)}$

$$\begin{aligned} R_{\tilde{\mathbf{X}}^{(N)}} &= E\left[\tilde{\mathbf{X}}^{(N)}\tilde{\mathbf{X}}^{(N)^T}\right] \\ &= \begin{bmatrix} \lambda_0^{(N)} & 0 & \ldots & 0 \\ 0 & \lambda_1^{(N)} & \ldots & 0 \\ \vdots & 0 & \ddots & 0 \\ 0 & 0 & \ldots & \lambda_{N-1}^{(N)} \end{bmatrix} \end{aligned} \tag{12}$$

where $\tilde{\mathbf{X}}^{(N)}$ is a Gaussian random vector whose elements are independent. Since $P^{(N)^T}\cdot P^{(N)} = I$, the measurement output can be rewritten as

$$\hat{\overline{\Gamma}}_L^{(N)} = \tilde{\mathbf{X}}^{(N)^T}\cdot\tilde{\mathbf{X}}^{(N)} + \tilde{\mathbf{Y}}^{(N)^T}\cdot\tilde{\mathbf{Y}}^{(N)}. \tag{13}$$

The probability density function of $\hat{\overline{\Gamma}}_L^{(N)}$ is determined by the characteristics of the eigenvalues $\left\{\lambda_0^{(N)},\ldots,\lambda_{N-1}^{(N)}\right\}$.

B. Toeplitz Forms

In order to determine the properties of the eigenvalues of the matrix $R_{\mathbf{X}^{(N)}}$, the standard theory of the asymptotic distribution of eigenvalues of Toeplitz forms is employed ([24]–[29]). Let

$$c_{i-j}^{(N)} = E\left[X_i^{(N)}X_j^{(N)}\right], \quad i,j=0,\ldots,N-1$$

where $E\left[X_i^{(N)}X_j^{(N)}\right]$ is determined by (7). Let $f^{(N)}(\omega)$ be a real-valued function such that

$$c_n^{(N)} = \frac{1}{2\pi}\int_{-\pi}^{\pi} e^{in\omega}f^{(N)}(\omega)d\omega, \quad n=0,\pm1,\ldots,\pm(N-1) \tag{14}$$

are its Fourier coefficients. Then,

$$\begin{aligned} f^{(N)}(\omega) &= \sum_{n=1-N}^{N-1} c_n^{(N)}e^{-jn\omega} \\ &= \frac{N_0}{N} + \frac{C^2}{2N}\sum_{n=-N+1}^{N-1} J_0(2\pi f_d nT_s)e^{-jn\omega} \end{aligned} \tag{15}$$

and

$$\begin{aligned} f^{(\infty)}(\omega) &\triangleq \lim_{N\to\infty} f^{(N)}(\omega=\Omega T_s) \\ &= \frac{C^2}{2T_m}\int_{-T_m}^{T_m} J_0(2\pi f_d\tau)e^{-j\Omega\tau}\,d\tau \\ &= \frac{C^2}{2T_m}\int_{-\infty}^{\infty} W(\tau)\,J_0(2\pi f_d\tau)\,e^{-j\Omega\tau}\,d\tau \end{aligned} \tag{16}$$

where

$$W(t) = \begin{cases} 1, & t\in[-T_m,T_m], \\ 0, & \text{otherwise.} \end{cases}$$

Since $R_{\mathbf{X}^{(N)}}$ is a real symmetric Toeplitz matrix, as $N\to\infty$, the eigenvalues of $R_{\mathbf{X}^{(N)}}$ are related to the set of values that $f^{(\infty)}(\omega)$ assumes on the sampling points between $[0,\pi]$[26]; that is, the sets $\{\lambda_n^{(N)},\ n=0,\ldots,N-1\}$ and $\left\{f^{(\infty)}\left(\frac{n\pi}{N}\right),\ n=0,\ldots,N-1\right\}$ are equally distributed, as $N\to\infty$, if [24], [25]

$$\lim_{N\to\infty}\sum_{n=-N+1}^{N-1}\left|c_n^{(N)}\right| < \infty \tag{17}$$

where the two sets $\left\{a_1^{(N)}, a_2^{(N)}, \ldots, a_N^{(N)}\right\}$ and $\left\{b_1^{(N)}, b_2^{(N)}, \ldots, b_N^{(N)}\right\}$, as $N \to \infty$, are equally distributed in the interval $[-K, K]$, with $\left|a_k^{(N)}\right| < K$ and $\left|b_k^{(N)}\right| < K$, $\forall\, k$, if the following condition holds [24]:

$$\lim_{N\to\infty} \frac{\sum_{k=1}^{N}\left[G\left(a_k^{(N)}\right) - G\left(b_k^{(N)}\right)\right]}{N} = 0$$

where $G(x)$ is an arbitrary continuous function in the interval $[-K, K]$. The condition in (17) is indeed satisfied

$$\begin{aligned}\lim_{N\to\infty} \sum_{n=-N+1}^{N-1} \left|c_n^{(N)}\right| &= \lim_{N\to\infty} \frac{C^2}{2N} \sum_{n=-N+1}^{N-1} |J_0(2\pi f_d n T_s)| \\ &= \frac{C^2}{2T_m} \int_{-T_m}^{T_m} |J_0(2\pi f_d \tau)| d\tau \\ &= \frac{C^2}{4\pi f_d T_m} \times \int_{-2\pi f_d T_m}^{2\pi f_d T_m} \left|\frac{1}{2\pi}\right. \\ &\quad \left. \int_{-\pi}^{\pi} \cos(z\sin\theta) d\theta\right| dz \\ &\le C^2 < \infty \end{aligned} \tag{18}$$

and thus the sets $\left\{\lambda_n^{(N)}, n=0,\ldots,N-1\right\}$ and $\left\{f^{(\infty)}\left(\frac{n\pi}{N}\right), n=0,\ldots,N-1\right\}$ are equally distributed in $(-\infty, \infty)$.

Letting $\Omega_d = 2\pi f_d$, the Fourier transform of (2) is given by

$$F[J_0(\Omega_d \tau)] = \begin{cases} \frac{2}{\sqrt{\Omega_d^2 - \Omega^2}}, & \text{if } |\Omega| \le \Omega_d \\ 0, & \text{otherwise} \end{cases} \tag{19}$$

and the Fourier transform of the truncated autocorrelation function is

$$F[W(\tau) J_0(\Omega_d \tau)] = \frac{2}{\pi} \int_{-\Omega_d}^{\Omega_d} \frac{1}{\sqrt{\Omega_d^2 - \mu^2}} \frac{\sin[T_m(\Omega - \mu)]}{(\Omega - \mu)} d\mu \tag{20}$$

and, by (16)

$$\begin{aligned} f^{(\infty)}(\omega) &\triangleq \lim_{N\to\infty} f^{(N)}(\omega = \Omega T_s) \\ &= \frac{C^2}{\pi} \int_{-\Omega_d}^{\Omega_d} \frac{1}{\sqrt{\Omega_d^2 - \mu^2}} \frac{\sin[T_m(\Omega - \mu)]}{T_m(\Omega - \mu)} d\mu. \end{aligned} \tag{21}$$

Note that $f^{(\infty)}(\omega)$ will have relevant support only on $[-\Omega_d T_s, \Omega_d T_s]$. Let $\left\{\lambda_n^{(\infty)}\right\}$ be the set of eigenvalues for the infinite correlation matrix of (11) when $N \to \infty$, which are equally distributed with the sample values that $f^{(\infty)}(\omega)$ assumes over $[0, \pi]$. The number of sampling points, $\lceil 2 f_d T_m \rceil$, which lie in $[0, \Omega_d T_s]$, is fixed by f_d and the window length T_m regardless of the sampling frequency. This implies that, as $N \to \infty$, a fixed number of eigenvalues will be playing the dominant role in determining the conditional probability density function $f_{\hat{\overline{\Gamma}}_L(t_0)|\overline{\Gamma}_L(t_0)}(x|y = C^2)$. This behavior will indeed be observed in succeeding sections.

C. Numerical Results and Interpretation

In this section, numerical results are presented to demonstrate that the previous analysis holds for even moderate values of N. The parameters used are: mobile speed $\nu = 40$ kmph, carrier frequency $f_c = 1$ GHz, $C^2 = 5.3$, $C^2/N_0 = 4.23$ dB, Doppler shift $f_d = \nu/\lambda = 37.03$ Hz. The measurement window is of duration $T_m = 85$ ms, and the sampling frequency will be given by $f_s = \beta f_d$. The properties of the eigenvalues of the matrix in (11) will be considered for various values of β. The numerical results are shown in Tables I and II. As expected, only a finite number M, where M is independent of N but subject to f_d and T_m, of the eigenvalues in the set $\left\{\lambda_k^{(N)} - (N_0/N)\right\}$ are nonzero. Thus, in (13), for large enough N, there are $(N - M)$ independent identically distributed (i.i.d.) Gaussian random variables in $\tilde{\mathbf{X}}^{(N)}$ whose variances are N_0/N. Per above, the M independent random variables corresponding to the first M eigenvalues are equally distributed with the sampling points of $f^{(\infty)}(\omega = \Omega T_s)$ in (21), as $N \to \infty$. Fig. 2 displays $f^{(\infty)}(\Omega)$, using the same parameters stated above.

These results demonstrate that for even moderate values of N, the second term in

$$\begin{aligned} \hat{\overline{\Gamma}}_L^{(N)} &= \sum_{k=0}^{M-1} \left[\left(\tilde{X}_k^{(N)}\right)^2 + \left(\tilde{Y}_k^{(N)}\right)^2\right] \\ &\quad + \sum_{k=M}^{N-1} \left[\left(\tilde{X}_k^{(N)}\right)^2 + \left(\tilde{Y}_k^{(N)}\right)^2\right] \end{aligned} \tag{22}$$

is the sum of i.i.d. random variables, $\left[\left(\tilde{X}_k^{(N)}\right)^2 + \left(\tilde{Y}_k^{(N)}\right)^2\right]$, each of which is exponentially distributed with mean $2N_0/N$. Thus, the second term has a chi-squared distribution with $2(N - M)$ degrees of freedom. The kth element in the first term of (22) is exponentially distributed with mean $\{2C^2\mu_k + 2N_0(1/N)\}$, where μ_k is solely dependent on f_d and T_m.

TABLE I
EIGENVALUES OF MATRIX $N \cdot R_{\mathbf{X}^{(N)}}$. PARAMETERS USED ARE: MOBILE SPEED $\nu = 40$ kmph, $f_c = 1$ GHz, $C^2 = 5.3$, $C^2/N_0 = 7.24$ dB, DOPPLER FREQUENCY SHIFT $f_d = \nu/\lambda = 37.03$ Hz. MEASUREMENT WINDOW IS OF DURATION $T_m = 85$ ms, AND SAMPLING FREQUENCY $f_s = \beta f_d$, $N = \lceil T_m/T_s \rceil$

$N\lambda_k^{(N)}$	(β, N, M)					
k	(20,63,10)	(67,211,10)	(71,224,10)	(80,252,10)	(200,630,10)	(450,1417,10)
0	36.6846	120.4892	127.6924	143.6827	357.6991	803.4813
1	34.9615	114.7786	121.7015	136.8748	340.6910	765.1473
2	22.0678	71.5643	75.7879	85.2571	211.6409	474.9272
3	21.2590	68.8556	72.9858	82.0330	203.5822	456.7136
4	16.7829	53.7771	57.2609	64.0658	158.6553	355.3005
5	18.2236	58.6929	62.1639	69.8907	173.2264	388.4777
6	18.6960	60.2793	63.8200	71.7814	177.9531	399.1421
7	5.6680	16.6555	17.9421	19.7469	47.8777	106.0456
8	1.5598	2.8964	3.0687	3.2739	6.6897	13.7313
9	1.0440	1.1513	1.1658	1.1816	1.4547	2.0166
10	1.0027	1.0094	1.0104	1.0113	1.0284	1.0635
$11 \sim N-1$	1.0000	1.0000	1.0000	1.0000	1.0000	1.0000

TABLE II
NORMALIZED EIGENVALUES OF MATRIX $R_{\mathbf{X}^{(N)}}$. PARAMETERS ARE THE SAME AS FOR TABLE I

$\lambda_k^{(N)} - \frac{N_0}{N}$	(β, N, M)					
k	(20,63,10)	(67,211,10)	(71,224,10)	(80,252,10)	(200,630,10)	(450,1417,10)
0	0.5664	0.5663	0.5656	0.5662	0.5662	0.5663
1	0.5391	0.5392	0.5388	0.5392	0.5392	0.5393
2	0.3344	0.3344	0.3339	0.3344	0.3344	0.3345
3	0.3216	0.3216	0.3214	0.3216	0.3216	0.3216
4	0.2505	0.2501	0.2512	0.2503	0.2502	0.2500
5	0.2734	0.2734	0.2731	0.2734	0.2734	0.2734
6	0.2809	0.2809	0.2804	0.2809	0.2809	0.2810
7	0.0741	0.0742	0.0756	0.0744	0.0744	0.0741
8	0.0089	0.0090	0.0092	0.0090	0.0090	0.0090
9	0.0007	0.0007	0.0007	0.0007	0.0007	0.0007
10	0.0000	0.0000	0.0000	0.0000	0.0000	0.0000
$11 \sim N-1$	0.0000	0.0000	0.0000	0.0000	0.0000	0.0000

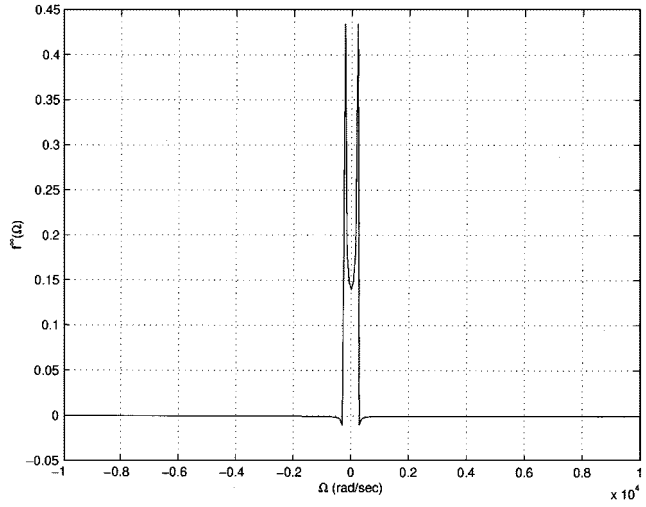

Fig. 2. Function $f^{(\infty)}(\Omega)$. Parameters used are: mobile speed $\nu = 40$ kmph, $f_c = 1$ GHz, $C^2 = 5.3$, $C^2/N_0 = 7.24$ dB, Doppler shift $f_d = \nu/\lambda = 37.03$ Hz. Measurement window is of duration $T_m = 85$ ms, and sampling frequency $f_s = \beta f_d$, $\beta = 200$, $N = \lceil T_m/T_s \rceil = 630$.

D. Asymptotic Conditional Distribution

Using the asymptotic properties of the eigenvalues $\left\{\lambda_n^{(N)}\right\}$, as discussed in Section III-C

$$\hat{\overline{\Gamma}}_L^{(N)} \stackrel{\mathcal{D}}{=} \sum_{k=0}^{M-1} W_k + W_{\text{noise}} \tag{23}$$

as $N \to \infty$, where $\stackrel{\mathcal{D}}{=}$ means equivalence in distribution. The set $\{W_k,\, k = 0,1,\ldots,M-1\}$ contains independent exponentially distributed random variables, and the kth element has probability density function

$$f_{W_k}(x) = \begin{cases} \tilde{\lambda}_k e^{-\tilde{\lambda}_k x}, & \text{if } x \geq 0 \\ 0, & \text{otherwise} \end{cases}$$

where

$$\frac{1}{\tilde{\lambda}_k} = 2\overline{\Gamma}_L \mu_k + 2N_0 \frac{T_s}{T_m}.$$

The term W_{noise} is a random variable caused by the additive noise, which, per Section III-C, has a chi-squared distribution with $2(\lceil T_m/T_s \rceil - M)$ degrees of freedom, where the variance of each component term is $N_0(T_s/T_m)$. By the central limit theorem (CLT) [30], W_{noise} will become normally distributed as $2(\lceil T_m/T_s \rceil - M) \to \infty$. However, by [32], the cube root transformation of a chi-squared random variable produces a much better approximation to normality when $2(\lceil T_m/T_s \rceil - M)$ is not large. Hence, let $Z = W_{\text{noise}}^{1/3}$. Now Z is approximately Gaussian-distributed [32] with mean

$$\mu_Z = \left(2N_0 \frac{T_s}{T_m}\right)^{1/3} \frac{\Gamma\left(\left\lceil \frac{T_m}{T_s} \right\rceil - M + \frac{1}{3}\right)}{\Gamma\left(\left\lceil \frac{T_m}{T_s} \right\rceil - M\right)} \tag{24}$$

and variance

$$\sigma_Z^2 = \left(2N_0 \frac{T_s}{T_m}\right)^{2/3} \left[\frac{\Gamma\left(\left\lceil \frac{T_m}{T_s} \right\rceil - M + \frac{2}{3}\right)}{\Gamma\left(\left\lceil \frac{T_m}{T_s} \right\rceil - M\right)} - \frac{\Gamma^2\left(\left\lceil \frac{T_m}{T_s} \right\rceil - M + \frac{1}{3}\right)}{\Gamma^2\left(\left\lceil \frac{T_m}{T_s} \right\rceil - M\right)}\right] \tag{25}$$

where $\Gamma(\cdot)$ is the Gamma function (36).

Then, the conditional distribution is given by

$$f_{\hat{\overline{\Gamma}}_L(t_0)|\overline{\Gamma}_L(t_0)}\left(x|\overline{\Gamma}_L(t_0) = \frac{1}{y}\right) = \sum_{k=0}^{M-1} \frac{y}{2} D_k e^{-\tilde{\lambda}_k x} B_k(x) \tag{26}$$

where

$$D_k = \left[\prod_{j=0, j\neq k}^{M-1} \frac{1}{\mu_k - \mu_j}\right] \left(\mu_k + N_0 \frac{T_s}{T_m} y\right)^{(M-2)}$$

and

$$B_k(x) = \int_0^{x^{1/3}} e^{\tilde{\lambda}_k t^3} \frac{1}{\sqrt{2\pi}\sigma_Z} e^{-(t-\mu_Z)^2/2\sigma_Z^2} dt.$$

IV. Optimal Power Control Schemes

A. Introduction

In this section, power control schemes, which are defined as maps from the noisy average power measurement to a transmission power, are considered. In particular, power control schemes are sought that are optimal in the sense that they minimize the average transmitted power to achieve a specified outage probability. For notational simplicity, throughout this section the shorthand $\overline{\Gamma}_L = \overline{\Gamma}_L(t_0 + \tau)$ and $\hat{\overline{\Gamma}}_L = \hat{\overline{\Gamma}}_L(t_0)$ will be employed for the shadowing at the time of interest and the shadowing estimate the system is employing, respectively.

For the single-user system, the average received signal-to-noise ratio (SNR) at the time of interest will be given by $\overline{\Gamma}_L \cdot \gamma$, where, per Section II-A, $\overline{\Gamma}_L^{-1}$ is log-normal distributed, and thus $-\ln \overline{\Gamma}_L \sim N(0, \sigma_Y^2)$ is Gaussian distributed after the normalization with mean $\mu = 0$, and γ is the ratio of the product of the transmitted power and path loss over the noise power. The transmitter and receiver design, channel fading assumptions, and quality-of-service (QoS) requirements fix a minimum required average SNR $\overline{\gamma}_0$ for acceptable system operation. Hence, the probability of outage will be defined as the probability that this average received SNR is not achieved; thus, the outage probability P_{outage} is given by the probability of the event $\{\overline{\Gamma}_L \cdot \gamma < \overline{\gamma}_0\}$. With the aim of compensating for the slow shadowing, the goal here is to develop a power control scheme $\gamma(x)$, which is the ratio of the product of the transmitted power and path loss over the noise power when $\hat{\overline{\Gamma}}_L = x$, to minimize the average transmitted power for a required outage probability P_{out}. Different models for the statistics of the measurement error yield different optimal power control schemes. The parameters to employ in (26) depend on the mobile speed, which can be well estimated [33], [34], and thus, these parameters will be assumed to be perfectly known in this paper. Robustness to uncertainties in the velocity estimates is relegated to future work. For simplicity of exposition, the case $\tau = 0$ is first considered through Section IV-D; then, the modifications for $\tau > 0$ are considered in Section IV-E.

B. Conventional Power Control Scheme

In conventional power control schemes, the estimation of the slow shadowing is generally regarded as perfect; in other words,

$\overline{\Gamma}_L = \hat{\overline{\Gamma}}_L$. For required outage probability P_{out}, the power control scheme that minimizes the average transmit power while meeting the outage probability constraint is given by [35]

$$\gamma_{\text{conv}}(x) = \begin{cases} \frac{\overline{\gamma}_0}{x}, & \text{if } x \geq X_{\text{conv}} \\ 0, & \text{otherwise} \end{cases} \tag{27}$$

where X_{conv} is the solution to

$$\int_0^{X_{\text{conv}}} f_{\overline{\Gamma}_L}(x)\,dx = P_{\text{out}}.$$

C. Optimal Power Control Scheme Under the Model of [10]

In [10], it is argued that the distribution of the actual shadowing given its estimate obtained by lowpass filtering is approximately distributed in a log-normal fashion; thus, $\hat{\overline{\Gamma}}_L = \overline{\Gamma}_L 10^{\delta/10}$, where δ, the estimation error in dB, is Gaussian distributed with mean 0 and standard deviation σ_0. The outage probability is given by

$$E_{\hat{\overline{\Gamma}}_L}[P_{\text{outage}}(x)] = \int_0^{\infty}\int_0^{\overline{\gamma}_0/\gamma(x)} f_{\overline{\Gamma}_L|\hat{\overline{\Gamma}}_L}(y|x)\cdot f_{\hat{\overline{\Gamma}}_L}(x)dydx. \tag{28}$$

Per above, the objective is to minimize the average transmission power

$$E_{\hat{\overline{\Gamma}}_L}[\gamma(x)] = \int_0^{\infty}\gamma(x)\cdot f_{\hat{\overline{\Gamma}}_L}(x)dx$$

subject to $E_{\hat{\overline{\Gamma}}_L}[P_{\text{outage}}(x)] \leq P_{\text{out}}$. This problem can be solved using the calculus of variations [31] to yield (29), as shown at the bottom of the page, where the unit of σ_0 and σ_Y here is Np and X_G is the solution to

$$1 - \int_{X_G}^{\infty} Q\left[\frac{\sigma_Y^2}{\sigma_0^2+\sigma_Y^2}\left(\sigma_0 - \sqrt{2\ln\frac{x}{X_G}}\right)\right]\cdot f_{\hat{\overline{\Gamma}}_L}(x)dx = P_{\text{out}}$$

where $Q(x) = \int_x^{\infty}(1/\sqrt{2\pi})e^{-t^2/2}dt$.

It should be noted that while solving the constrained optimization problem stated above, there is a root ambiguity in the sense that there are two possible power control solutions. The second possible power control function is given by (30), as shown at the bottom of the page. However, in this case, the corresponding outage probability cannot be made arbitrarily small as required

$$\begin{aligned} P_{\text{outage}} &= 1 - \int_{X_G}^{\infty} Q\left[\frac{\sigma_Y^2}{\sigma_0^2+\sigma_Y^2}\left(\sigma_0 + \sqrt{2\ln\frac{x}{X_G}}\right)\right] f_{\hat{\overline{\Gamma}}_L}(x)dx \\ &\geq 1 - \frac{1}{2}\int_{X_G}^{\infty} f_{\hat{\overline{\Gamma}}_L}(x)dx \\ &\geq \frac{1}{2}. \end{aligned} \tag{31}$$

Thus, this second solution is discarded.

D. Optimal Power Control Scheme Under (26)

Using the accurate measurement error statistics of (26), an optimal power control algorithm can be developed by solving the following constrained optimization problem:

$$\begin{aligned} \gamma_{new}(x) &= \arg\min_{\gamma(x)} E_{\hat{\overline{\Gamma}}_L}[\gamma(x)] \\ &= \arg\min_{\gamma(x)} \int_0^{\infty}\int_0^{\infty} \gamma(x) f_{\overline{\Gamma}_L^{-1}}(y) \\ &\quad \times f_{\hat{\overline{\Gamma}}_L|\overline{\Gamma}_L^{-1}}(x|y)dydx \end{aligned} \tag{32}$$

subject to

$$\begin{aligned} E_{\hat{\overline{\Gamma}}_L}[P_{\text{outage}}(x)] = \int_0^{\infty}\int_{\gamma(x)/\overline{\gamma}_0}^{\infty} & f_{\overline{\Gamma}_L^{-1}}(y) \\ & \times f_{\hat{\overline{\Gamma}}_L|\overline{\Gamma}_L^{-1}}(x|y)dydx \leq P_{\text{out}} \end{aligned} \tag{33}$$

where $f_{\overline{\Gamma}_L^{-1}}(y)$ and $f_{\hat{\overline{\Gamma}}_L|\overline{\Gamma}_L^{-1}}(x|y)$ are the marginal distribution function of $\overline{\Gamma}_L^{-1}$, and the conditional distribution function of $\hat{\overline{\Gamma}}_L$ given $\overline{\Gamma}_L^{-1}$, respectively.

This constrained optimization problem above can again be solved by referring to the calculus of variations [31]. The solution $\gamma(x)$ is the root of the following nonlinear equation involving the parameter λ, which is determined by the outage probability requirement in (33):

$$\frac{\overline{\gamma}_0}{\lambda} f_{\hat{\overline{\Gamma}}_L}(x) = f_{\overline{\Gamma}_L^{-1}}(y) f_{\hat{\overline{\Gamma}}_L|\overline{\Gamma}_L^{-1}}(x|y)|_{y=\gamma(x)/\overline{\gamma}_0} \tag{34}$$

$$f_{\hat{\overline{\Gamma}}_L}(x) = \int_0^{\infty} f_{\overline{\Gamma}_L^{-1}}(y) f_{\hat{\overline{\Gamma}}_L|\overline{\Gamma}_L^{-1}}(x|y)dy. \tag{35}$$

While solving for $\gamma(x)$ in (34) numerically, the smaller root will be discarded for the same reason stated in Section IV-C. Unlike

$$\gamma_G(x) = \begin{cases} \overline{\gamma}_0 \cdot \exp\left[\frac{\sigma_Y^2}{\sigma_0^2+\sigma_Y^2}\left(\sigma_0\sqrt{2\ln\frac{x}{X_G}} - \sigma_0^2 - \ln x\right)\right], & \text{if } x \geq X_G \\ 0, & \text{otherwise} \end{cases} \tag{29}$$

$$\gamma_G(x) = \begin{cases} \overline{\gamma}_0 \cdot \exp\left[\frac{\sigma_Y^2}{\sigma_0^2+\sigma_Y^2}\left(-\sigma_0\sqrt{2\ln\frac{x}{X_G}} - \sigma_0^2 - \ln x\right)\right], & \text{if } x \geq X_G \\ 0, & \text{otherwise} \end{cases} \tag{30}$$

in Section IV-C, we are unable to get a closed-form power control rule here. Thus, the new power control function based on the proposed conditional probability function in (26) is derived numerically.

E. Extensions to the $\tau > 0$ Case

In most practical applications, there will be appreciable delay between the time the shadowing estimate is made and the time the estimate is employed for system adjustments. Without loss of generality, t_0 is set to be zero. Then given the measurements of the shadowing at time t_0, the average outage probability of the event $\{\overline{\Gamma}_L(t_0+\tau)\cdot\gamma(x) < \overline{\gamma}_0\}$ at $t_0+\tau$ will be

$$E_{\hat{\overline{\Gamma}}_L}[P_{\text{outage}}(x,\tau)] = \int_0^\infty \int_{\gamma(x)/\overline{\gamma}_0}^\infty f_{\overline{\Gamma}_L^{-1}(\tau),\hat{\overline{\Gamma}}_L(0)}(z,x)\,dz\,dx \tag{36}$$

where the joint distribution $f_{\overline{\Gamma}_L^{-1}(\tau),\hat{\overline{\Gamma}}_L(0)}(z,x)$ is determined by

$$f_{\overline{\Gamma}_L^{-1}(\tau),\hat{\overline{\Gamma}}_L(0)}(z,x) = \int_0^\infty f_{\hat{\overline{\Gamma}}_L(0)|\overline{\Gamma}_L^{-1}(0)}(x|y) \cdot f_{\overline{\Gamma}_L^{-1}(0),\overline{\Gamma}_L^{-1}(\tau)}(y,z)\,dy. \tag{37}$$

The quantities $\ln\overline{\Gamma}_L^{-1}(0)$ and $\ln\overline{\Gamma}_L^{-1}(\tau)$ are jointly Gaussian random variables, with zero mean and standard deviation σ_Y. The correlation coefficient between them is $\rho = e^{-\nu|\tau|/X_c}$, as in (3). By solving the following constrained optimization problem:

$$\gamma_{new}(x) = \arg\min_{\gamma(x)} E_{\hat{\overline{\Gamma}}_L}[\gamma(x)] \tag{38}$$

subject to

$$E_{\hat{\overline{\Gamma}}_L}[P_{\text{outage}}(x,\tau)] \le P_{\text{out}}$$

conditional distribution functions $f_{\hat{\overline{\Gamma}}_L(0)|\overline{\Gamma}_L^{-1}(0)}(x|y)$ in [10] and (26) will produce new power control schemes for the case $\tau > 0$.

Using the same arguments as in Section IV-C, the optimal power control scheme under [10] for $\tau > 0$ is given by (39), as shown at the bottom of the page, where $\alpha = 1 + (\sigma_Y^2/\sigma_0^2)(1-\rho^2)$ and X_{GD} is the solution of

$$1 - \int_{X_{GD}}^\infty Q\left[\frac{\sigma_Y^2}{\sigma_0^2+\sigma_Y^2}\left(\sqrt{\alpha}\sigma_0 - \sqrt{2\rho\ln\frac{x}{X_{GD}}}\right)\right] \cdot f_{\hat{\overline{\Gamma}}_L}(x)\,dx = P_{\text{out}}.$$

It is easily verified that (29) is the special case of (39), when $\tau = 0$ (and thus $\rho = 1$).

The optimal power control scheme under (26) can be developed numerically as was done in Section IV-D, which results in

$$\frac{\overline{\gamma}_0}{\lambda} f_{\hat{\overline{\Gamma}}_L(0)}(x) = f_{\overline{\Gamma}_L^{-1}(\tau),\hat{\overline{\Gamma}}_L(0)}(z,x)\big|_{z=\gamma(x)/\overline{\gamma}_0}$$
$$f_{\hat{\overline{\Gamma}}_L(0)}(x) = \int_0^\infty f_{\overline{\Gamma}_L^{-1}(0)}(y) f_{\hat{\overline{\Gamma}}_L(0)|\overline{\Gamma}_L^{-1}(0)}(x|y)\,dy \tag{40}$$

where λ is chosen to make $E_{\hat{\overline{\Gamma}}_L}[P_{\text{outage}}(x,\tau)] = P_{\text{out}}$.

F. Comparison of Power Control Schemes

1) Numerical Results: Optimal power control rules derived under (26) will be compared to those obtained from the conventional method and under the model of [10]. However, since the previous models are only approximations, power control rules based on previous models will not meet the prescribed outage probability constraint. Thus, an energy margin is added to each of the suboptimal rules to yield the modified rules as shown in (41)–(43) at the bottom of the page, where M_G, M_{conv} and M_{GD} are chosen to meet the outage probability constraint (33) under (26) by replacing $\gamma(x)$ in (33) with $\tilde{\gamma}_G(x)$, $\tilde{\gamma}_{\text{conv}}(x)$, and $\tilde{\gamma}_{GD}(x)$, respectively.

The parameters used in the numerical results are $P_{\text{out}} = 0.01$, $\nu = 40$ kmph, $f_c = 1$ GHz, $\sigma_Y = 8$ dB, and $\sigma_0 = 2.7$ dB, where σ_0 in (41) is the measurement error (in Np), σ_Y is the standard deviation of the shadowing in ln scale as defined in [10]. The mobile speed and the carrier frequency are 40 kmph and 1 GHz, respectively, the measurement window length is $T_m = 85$ ms, and the symbol rate is $1/T_s = 10$ kHz. The ratio of the effective correlation distance of shadowing over the wavelength is $(X_c/\lambda) = 40$. Under these conditions, the

$$\gamma_{GD}(x) = \begin{cases} \overline{\gamma}_0 \cdot \exp\left[\frac{\sigma_Y^2}{\sigma_0^2+\sigma_Y^2}\left(\sqrt{\alpha}\sigma_0\sqrt{2\rho\ln\frac{x}{X_{GD}}} - \sigma_0^2\alpha - \rho\ln x\right)\right], & \text{if } x \ge X_{GD} \\ 0, & \text{otherwise} \end{cases} \tag{39}$$

$$\tilde{\gamma}_G(x) = \begin{cases} M_G \cdot \overline{\gamma}_0 \cdot \exp\left[\frac{\sigma_Y^2}{\sigma_0^2+\sigma_Y^2}\left(\sigma_0\sqrt{2\ln\frac{x}{X_G}} - \sigma_0^2 - \ln x\right)\right], & \text{if } x \ge X_G \\ 0, & \text{otherwise} \end{cases} \tag{41}$$

$$\tilde{\gamma}_{\text{conv}}(x) = \begin{cases} M_{\text{conv}} \cdot \frac{\overline{\gamma}_0}{x}, & \text{if } x \ge X_{\text{conv}}, \\ 0, & \text{otherwise} \end{cases} \tag{42}$$

$$\tilde{\gamma}_{GD}(x) = \begin{cases} M_{GD} \cdot \overline{\gamma}_0 \cdot \exp\left[\frac{\sigma_Y^2}{\sigma_0^2+\sigma_Y^2}\left(\sqrt{\alpha}\sigma_0\sqrt{2\rho\ln\frac{x}{X_{GD}}} - \alpha\sigma_0^2 - \rho\ln x\right)\right], & \text{if } x \ge X_{GD} \\ 0, & \text{otherwise} \end{cases} \tag{43}$$

TABLE III
PARAMETERS FOR NUMERICAL RESULTS ARE: $\nu = 40$ kmph, $f_c = 1$ GHz, $\sigma_Y = 8$ dB, $\sigma_0 = 2.7$ dB, $T_m = 85$ ms, $T_s = 1/(10$ kHz$)$. UNDER THESE CONDITIONS, THRESHOLDS ARE GIVEN BY $X_G = -27.45$ dB, $X_{\rm conv} = -18.62$ dB. AVERAGE TRANSMIT POWER AND OUTAGE PROBABILITY OF POWER CONTROL RULES IN (32), (29), AND (27) ARE SHOWN AS "NEW MODEL", "LOGN", AND "CONV", RESPECTIVELY, UNDER (26), FOR THREE DIFFERENT CASES ($\overline{\gamma}_0 = 26.98$ dB, 16.90 DB, 6.79 DB). ENERGY MARGINS M_G AND $M_{\rm conv}$ IN (41) AND (42) ARE CALCULATED SO THAT SUBOPTIMAL POWER CONTROL SCHEMES MEET OUTAGE PROBABILITY REQUIREMENTS, AND PERFORMANCE OF MODIFIED SUBOPTIMAL POWER CONTROL RULES (41) AND (42) ARE SHOWN IN COLUMNS "MODI LOGN" AND "MODI CONV", RESPECTIVELY. PARENTHESES PARTS "()" IN THE COSTS OF NON-EXACT MODELS AFTER ADDING POWER MARGINS IN (41) AND (42): HOW MUCH MORE AVERAGE POWER THAN THAT OF "NEW MODEL" WILL BE NEEDED TO MEET AVERAGE OUTAGE PROBABILITY REQUIREMENTS

With additive noise in the measurement, $\overline{\gamma}_0 =$ 26.98 dB					
	New Model	LogN	Modi LogN	Conv	Modi Conv
P_{out}	1.00e-2	6.83e-3	1.00e-2	4.67e-1	9.95e-3
P_{av}(dB)	36.36	37.76	37.19(0.83)	33.05	37.10(0.74)
Margin(dB)	0.00	0.00	-0.56	0.00	4.05
Without additive noise in the measurement, $\overline{\gamma}_0 =$ 26.98 dB					
	New Model	LogN	Modi LogN	Conv	Modi Conv
P_{out}	1.00e-2	3.76e-3	1.00e-2	4.49e-1	1.00e-2
P_{av}(dB)	36.37	38.02	36.88(0.51)	33.94	37.42(1.05)
Margin(dB)	0.00	0.00	-1.14	0.00	3.48
With additive noise in the measurement, $\overline{\gamma}_0 =$ 16.90 dB					
	New Model	LogN	Modi LogN	Conv	Modi Conv
P_{out}	1.00e-2	2.74e-2	1.00e-2	5.70e-1	1.00e-2
P_{av}(dB)	26.28	26.44	28.91(2.63)	21.30	27.36(1.08)
Margin(dB)	0.00	0.00	2.47	0.00	6.06
Without additive noise in the measurement , $\overline{\gamma}_0 =$ 16.90 dB					
	New Model	LogN	Modi LogN	Conv	Modi Conv
P_{out}	1.00e-2	3.76e-3	1.00e-2	4.49e-1	1.00e-2
P_{av}(dB)	26.30	27.94	26.80(0.50)	23.86	27.34(1.04)
Margin(dB)	0.00	0.00	-1.14	0.00	3.48
With additive noise in the measurement , $\overline{\gamma}_0 =$ 6.79 dB					
	New Model	LogN	Modi LogN	Conv	Modi Conv
P_{out}	1.00e-2	1.29e-1	1.00e-2	7.96e-1	9.99e-3
P_{av}(dB)	16.34	13.24	22.09(5.75)	6.33	21.31(4.97)
Margin(dB)	0.00	0.00	8.85	0.00	14.99
Without additive noise in the measurement , $\overline{\gamma}_0 =$ 6.79 dB					
	New Model	LogN	Modi LogN	Conv	Modi Conv
P_{out}	1.00e-2	3.76e-3	1.00e-2	4.49e-1	1.00e-2
P_{av}(dB)	16.19	17.83	16.69(0.50)	13.75	17.23(1.04)
Margin(dB)	0.00	0.00	-1.14	0.00	3.48

thresholds for the case when there is no time delay between the measurement and its use are $X_{\rm conv} = -18.62$ dB and $X_G = -27.45$ dB. For cases taking into account the time delay between the measurements and power adjustments, the thresholds in (39) are $X_{GD} = -28.09$ dB for $\tau = 10$ ms, $\rho = 0.99$, $X_{GD} = -33.55$ dB for $\tau = 100$ ms, $\rho = 0.91$, and $X_{GD} = -42.53$ dB for $\tau = 250$ ms, $\rho = 0.79$.

In Table III the average transmit power and the outage probability of the power control rules in (32), (29), and (27) are shown as "New model," "LogN," and "Conv," respectively, under (26), for three different cases ($\overline{\gamma}_0 = 26.98$ dB, 16.90 dB, 6.79 dB). Per above, the energy margins M_G and $M_{\rm conv}$ in (41) and (42) are then calculated so that the power control schemes based on the previous models meet the outage probability requirements, and the performance of the modified suboptimal power control rules (41) and (42) are shown in columns "Modi LogN" and "Modi Conv," respectively. To see the impact of the additive noise *in the measurement* on the performance of various power control rules, the power control rules are compared with and without additive noise in the measurement. Without additive noise in the measurement, the term $B_k(x)$ is equal to 1 and $N_0 = 0$ in (26).

TABLE IV
WHEN SAMPLE SIZE IS LARGE ENOUGH, $W_{\rm noise}$ TERM IN (23) CAN BE APPROXIMATED AS CONSTANT. PARAMETERS ARE THE SAME AS FOR TABLE III. PARENTHESES "()" IN LOSSES WHEN EMPLOYING ARE OF THE NONEXACT MODELS AFTER ADDING POWER MARGINS IN (41) AND (42)

W_{noise} removed, $\overline{\gamma}_0 =$ 26.98 dB					
	New Model	LogN	Modi LogN	Conv	Modi Conv
P_{out}	1.00e-2	3.80e-3	1.00e-2	4.50e-1	1.00e-2
P_{av}(dB)	36.38	38.02	36.89(0.51)	33.94	37.42(1.04)
Margin(dB)	0.00	0.00	-1.13	0.00	3.48
W_{noise} removed, $\overline{\gamma}_0 =$ 16.90 dB					
	New Model	LogN	Modi LogN	Conv	Modi Conv
P_{out}	1.00e-2	4.11e-3	1.00e-2	4.52e-1	1.00e-2
P_{av}(dB)	26.30	27.92	26.85(0.55)	23.83	27.32(1.02)
Margin(dB)	0.00	0.00	-1.07	0.00	3.49
W_{noise} removed ,$\overline{\gamma}_0 =$ 6.79 dB					
	New Model	LogN	Modi LogN	Conv	Modi Conv
P_{out}	1.00e-2	7.26e-3	1.00e-2	4.67e-1	1.00e-2
P_{av}(dB)	16.39	17.58	17.09(0.70)	13.44	17.02(0.63)
Margin(dB)	0.00	0.00	-0.49	0.00	3.58

If the sample size $\lceil T_m/T_s \rceil$ is large enough, the variance (25) of $W_{\rm noise}^{1/3}$ is so small (7.3×10^{-5} under the parameters set above for $\overline{\gamma}_0 = 6.79$ dB) that the $W_{\rm noise}$ term in (23) can be approximated as constant and depends only on N_0 after normalization. Thus, it can be removed from the measurement $\hat{\overline{\Gamma}}_L^{(N)}$, and the conditional distribution function (26) can be modified accordingly. In Table IV, the average outage probability and average power of the schemes in (32), (29), and (27) are recalculated using this modified measurement model for cases: $\overline{\gamma}_0 = 26.98$ dB, 16.90 dB, 6.79 dB. Under this modified model, M_G and $M_{\rm conv}$ in (41) and (42) are determined to meet the outage probability requirements.

In Table V, time delay between the measurement and its employment is considered. The performances of power control schemes in (40), (29), (41), (39), and (43) are listed as " New $\rm Model_D$," "LogN," "Modi LogN," "$\rm LogN_D$," and "Modi $\rm LogN_D$," respectively, in terms of the average outage probability, average power, and the power margins, for cases of different time delays τ and whether the $W_{\rm noise}$ term in (23) is removed or kept. The threshold X_G in (29) is -27.45 dB, X_{GD} in (39) is -28.09 dB, -33.55 dB, and -42.53 dB for $\tau = 10$ ms, 100 ms, and 250 ms, respectively, when $\overline{\gamma}_0 = 6.79$ dB.

When $\overline{\gamma}_0 = 6.79$ dB, the marginal distribution of the measurement of the average power is shown in Fig. 3. Power control functions under the various models are shown in Figs. 4 and 5.

2) Discussion: From Table III, when $W_{\rm noise}$ is not removed, it is apparent that the accurate expression derived in this paper for the statistics of the error in the average power measurement does have an impact on system design. This difference is due to two effects: 1) the correlation of the samples employed in the average power measurement, and 2) the additive noise in the average power measurement. First, consider the case where there is no additive noise at the input to the measurement filter, which was an assumption in [10] that helped lead to their model. From Table III, it is apparent that the gain obtained by employing power control functions based on the accurate expression in (26) over the power control function based on the model of [10] is less than 0.5 dB for this case, whereas the gain over the conventional power control function can be on the order of

TABLE V

PARAMETERS ARE THE SAME AS IN TABLE III. RATIO OF EFFECTIVE CORRELATION DISTANCE OF SHADOWING X_c OVER WAVELENGTH λ IS $X_c/\lambda = 40$. PERFORMANCES OF POWER CONTROL SCHEMES IN (40), (29), (41), (39), AND (43) ARE LISTED AS "$\mathrm{New\ Model}_D$," "LOGN," "MODI LOGN," "LogN_D," AND "$\mathrm{ModiLogN}_D$," RESPECTIVELY, IN TERMS OF AVERAGE OUTAGE PROBABILITY, AVERAGE POWER, AND POWER MARGINS, IN CASES OF DIFFERENT TIME DELAYS τ, AND WHETHER W_{noise} TERM IN (23) IS REMOVED OR KEPT. THRESHOLD X_G IN (29) IS -27.45 dB. X_{GD} IN (29) ARE -28.09 dB, -33.55 dB, -42.53 dB FOR $\tau = 10$ ms, 100 MS, AND 250 MS, RESPECTIVELY, WHEN $\overline{\gamma}_0 = 6.79$ dB. PARENTHESES PARTS "()" IN COSTS OF NONEXACT MODELS AFTER ADDING POWER MARGINS IN (41) AND (43)

W_{noise} removed, $\tau = 10$ ms, $\rho = 0.99$, $\overline{\gamma}_0 = 6.79$ dB					
	New Model$_D$	LogN	Modi LogN	LogN$_D$	Modi LogN$_D$
P_{out}	1.00e-2	8.46e-3	1.00e-2	7.40e-3	1.00e-2
P_{av}(dB)	16.81	17.58	17.33(0.52)	17.89	17.44(0.63)
Margin(dB)	0.00	0.00	-0.25	0.00	-0.45
W_{noise} kept, $\tau = 10$ ms, $\rho = 0.99$, $\overline{\gamma}_0 = 6.79$ dB					
	New Model$_D$	LogN	Modi LogN	LogN$_D$	Modi LogN$_D$
P_{out}	9.99e-3	1.30e-1	9.99e-3	1.17e-1	1.00e-2
P_{av}(dB)	16.65	13.24	22.07(5.42)	13.73	22.13(5.48)
Margin(dB)	0.00	0.00	8.83	0.00	8.40
W_{noise} removed, $\tau = 100$ ms, $\rho = 0.91$, $\overline{\gamma}_0 = 6.79$ dB					
	New Model$_D$	LogN	Modi LogN	LogN$_D$	Modi LogN$_D$
P_{out}	9.97e-3	3.18e-2	1.00e-2	8.65e-3	1.00e-2
P_{av}(dB)	19.37	17.58	19.48(0.11)	19.85	19.59(0.22)
Margin(dB)	0.00	0.00	1.90	0.00	-0.26
W_{noise} kept, $\tau = 100$ ms, $\rho = 0.91$, $\overline{\gamma}_0 = 6.79$ dB					
	New Model$_D$	LogN	Modi LogN	LogN$_D$	Modi LogN$_D$
P_{out}	9.96e-3	1.48e-1	1.00e-2	6.28e-2	1.00e-2
P_{av}(dB)	19.57	13.24	22.17(2.60)	16.69	22.61(3.04)
Margin(dB)	0.00	0.00	8.93	0.00	5.92
W_{noise} removed, $\tau = 250$ ms, $\rho = 0.79$, $\overline{\gamma}_0 = 6.79$ dB					
	New Model$_D$	LogN	Modi LogN	LogN$_D$	Modi LogN$_D$
P_{out}	1.00e-2	7.84e-2	1.00e-2	9.25e-3	1.00e-2
P_{av}(dB)	21.30	17.58	22.20(0.90)	21.68	21.51(0.21)
Margin(dB)	0.00	0.00	4.62	0.00	-0.17
W_{noise} kept, $\tau = 250$ ms, $\rho = 0.79$, $\overline{\gamma}_0 = 6.79$ dB					
	New Model$_D$	LogN	Modi LogN	LogN$_D$	Modi LogN$_D$
P_{out}	1.00e-2	1.80e-1	1.00e-2	3.48e-2	9.99e-3
P_{av}(dB)	21.97	13.24	22.50(0.53)	19.41	23.21(1.24)
Margin(dB)	0.00	0.00	9.26	0.00	3.80

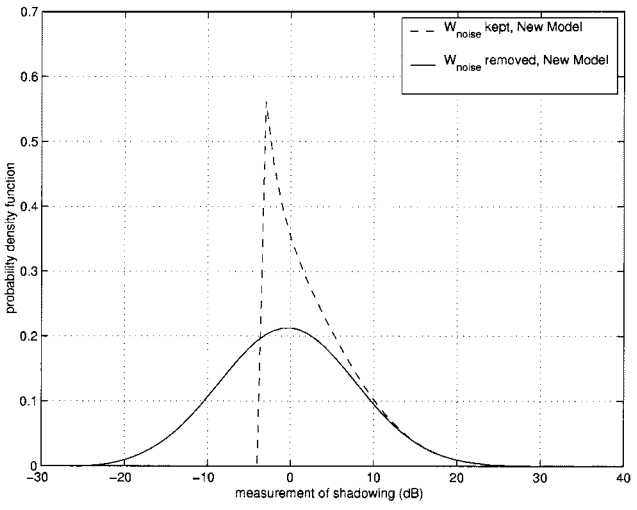

Fig. 3. Marginal probability density function of shadowing measurement (in dB) in cases with W_{noise} kept and W_{noise} removed. Parameters are $\nu = 40$ kmph, $f_c = 1$ GHz, $\sigma_Y = 8$ dB, $\sigma_0 = 2.7$ dB, $T_m = 85$ ms, $T_s = 1/(10\ \mathrm{KHz})$, SNR $= \overline{\gamma}_0 = 6.79$ dB.

1.0 dB. When measurement noise is considered, it is apparent from Table III that the model of [10] leads to a distinctly suboptimal power control rule. In particular, the loss at a required

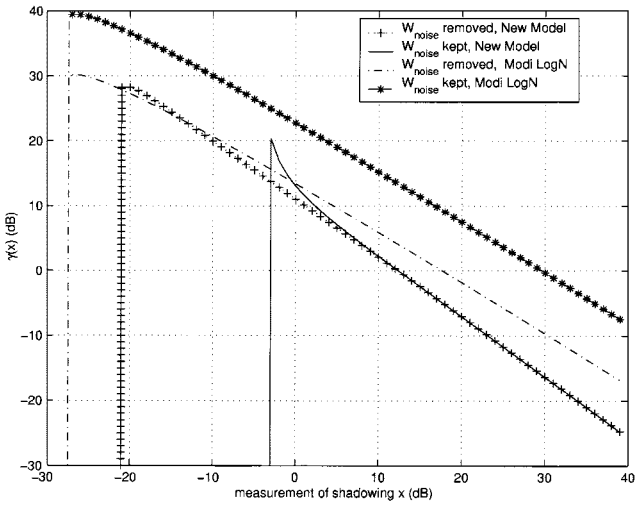

Fig. 4. Power control function (34) under model (26) and power control function (41) under the measurement error model in [10] with margin M_G, when path loss information is known and unknown in the case with additive noise in the measurement and time delay $\tau = 0$, $\rho = 1.0$. Parameters are $\nu = 40$ kmph, $f_c = 1$ GHz, $\sigma_Y = 8$ dB, $\sigma_0 = 2.7$ dB, $T_m = 85$ ms, $T_s = 1/(10\ \mathrm{kHz})$, SNR $= \overline{\gamma}_0 = 6.79$ dB, $X_G = -27.45$ dB.

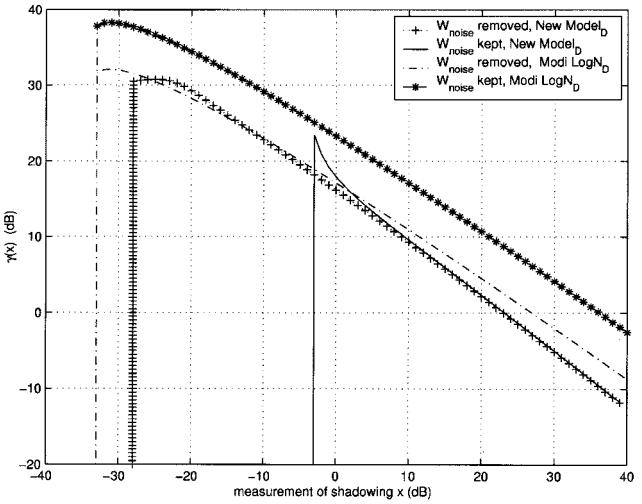

Fig. 5. Power control function (40) under the model (26), and power control function (43) under the measurement error model in [10] with margin M_{GD}, when path loss information is known and unknown in the case with additive noise in the measurement and time delay $\tau = 100$ ms, $\rho = 0.91$. Parameters are $\nu = 40$ kmph, $f_c = 1$ GHz, $\sigma_Y = 8$ dB, $\sigma_0 = 2.7$ dB, $T_m = 85$ ms, $T_s = 1/(10\ \mathrm{kHz})$, SNR $= \overline{\gamma}_0 = 6.79$ dB, $X_{GD} = -33.55$ dB.

average received SNR of 6.79 dB can be over 3 dB versus the power control rule based on (26). This is a significant loss that demonstrates the impact that the accurate model of (26) may have on wireless system design and analysis. However, as shown in Table IV, when the W_{noise} term in (23) is removed, then the gain obtained by employing power control functions based on the accurate expression in (26) over the power control function based on the model of [10] after adding the power margins are less than 1.0 dB.

From Table V, the impact of the time delay between the instants when the shadowing measurement has been made and when the power is adjusted can be seen. If W_{noise} is removed from $\hat{\overline{\Gamma}}_L^{(N)}$ in (23), the gains of the power control scheme (40)

"New Model$_D$" over "Modi LogN$_D$" (43) are decreasing from 0.63 dB to 0.21 dB, as time delay τ increases from 10 ms to 250 ms, ρ decreases from 0.99 to 0.79. This is due to the fact that as τ is increasing, the correlation of the log-normal shadowing is decreasing, and the information provided by the measurements of the average power outdated by τ will be decreasing. In the limiting case, as $\tau \to \infty$, the outdated measurement reveals nothing about the current shadowing and the power control schemes will be the same.

V. Conclusions

In this paper, the error statistics for average power measurements have been considered; in particular, the probability distribution of the value of the average received power at the time of interest conditioned on an outdated measurement has been obtained. To demonstrate its utility, this expression has been employed in the design of power control algorithms that minimize the average transmitted power required to achieve a desired outage probability for the link. It is demonstrated that power control algorithms based on the accurate expression derived in this paper can demonstrate gains in certain situations over those based on previous approximate models. This accurate characterization of the error statistics in average power measurements should also prove useful in the design and analysis of the multitude of other algorithms that rely on average received power measurements. Since the conditional probability distribution of the value of the average received power at the time of interest conditioned on an outdated measurement is subject to the correlation model used for the small scale fading (2) and the correlation model of the log-normal shadowing (3), if the actual correlation models do not agree with the assumed models of (2) and (3), the statistical model (26) has to be modified accordingly in a straightforward manner. In the case of design, such as that of the power control schemes considered in the latter part of this paper, the robustness to deviations of the correlation models from the assumed ones will be a topic of future research.

Acknowledgment

The authors are indebted to K. Chugg and M. Fitz, whose questions on modeling issues at the Thirty-Third Asilomar Conference on Signals, Systems, and Computers motivated a large portion of this work. The authors are grateful to three anonymous reviewers whose comments greatly improved the first version of this paper.

References

[1] A. Goldsmith and S. Chua, "Variable-rate variable-power MQAM for fading channels," *IEEE Trans. Commun.*, vol. 45, pp. 1218–1230, Oct. 1997.

[2] ——, "Adaptive coded modulation for fading channels," *IEEE Trans. Commun.*, vol. 46, pp. 595–602, May 1998.

[3] D. Goeckel, "Adaptive coding for time-varying channels using outdated fading estimates," *IEEE Trans. Commun.*, vol. 47, pp. 844–855, June 1999.

[4] S. Nanda, K. Balachandran, and S. Kumar, "Adaptation techniques in wireless packet data services," *IEEE Commun. Mag.*, pp. 54–64, Jan. 2000.

[5] F. Santucci, W. Huang, and V. Bhargava, "A framework for analyzing the user membership in cellular CDMA networks," *IEEE Trans. Commun.*, pp. 442–454, Mar. 2000.

[6] V. Veeravalli and O. Kelly, "A locally optimal handoff algorithm for cellular communications," *IEEE Trans. Veh. Technol.*, pp. 603–609, Aug. 1997.

[7] A. J. Viterbi, A. M. Viterbi, K. Gilhousen, and E. Zehavi, "Soft handoff extends CDMA cell coverage and increases reverse-link capacity," *IEEE J. Select. Areas Commun.*, pp. 1281–1288, Oct. 1994.

[8] J. Zander, "Performance of optimum transmitter power control in cellular radio systems," *IEEE Trans. Veh. Technol.*, pp. 57–62, Feb. 1992.

[9] A. Monk and L. Milstein, "Open-loop power control error in a land mobile satellite system," *IEEE J. Select. Areas Commun.*, pp. 205–212, Feb. 1995.

[10] A. Goldsmith, L. Greenstein, and G. Foschini, "Error statistics of real-time power measurements in cellular channels with multipath and shadowing," *IEEE Trans. Veh. Technol.*, vol. 43, pp. 439–446, Aug. 1994.

[11] A. Goldsmith and L. Greenstein, "Effects of average power estimation error on adaptive MQAM modulation," in *Proc. ICC'97*, Montreal, PQ, Canada, pp. 1105–1109.

[12] R. Yates, "A framework for uplink power control in cellular radio systems," *IEEE J. Select. Areas Commun.*, vol. 13, pp. 1341–1347, Sept. 1995.

[13] S. Ulukus and R. Yates, "Stochastic power control for cellular radio systems," *IEEE Trans. Commun.*, vol. 46, pp. 784–798, June 1998.

[14] S. Wei and D. Goeckel, "Adaptive signaling based on measurements with statistical uncertainty," in *Proc. 33rd Asilomar Conf. on Signals, Systems, and Computers*, vol. 1, Pacific Grove, CA, 1999, pp. 27–31.

[15] J. Proakis, *Digital Communications*, Third ed. New York: McGraw-Hill, 1995.

[16] W. Lee, *Mobile Communications Engineering*. New York: McGraw-Hill, 1998.

[17] W. C. Jakes, Ed., *Microwave Mobile Communications*. New York: IEEE Press, 1994.

[18] P. Bello, "Characterization of randomly time-variant linear channels," *IEEE Trans. Commun. Technol.*, vol. COM–11, pp. 360–393, Dec. 1963.

[19] M. Gudmundson, "Correlation model for shadow fading in mobile radio systems," *Electron. Lett.*, vol. 27, pp. 2145–2146, Nov. 1991.

[20] W. Lee and Y. Yeh, "On the estimation of the second-order statistics of log-normal fading in mobile radio environment," *IEEE Trans. Commun.*, pp. 869–873, June 1974.

[21] W. Lee, "Estimate of local average power of a mobile radio signal," *IEEE Trans. Veh. Technol.*, pp. 22–27, Feb. 1985.

[22] D. Wong and D. Cox, "Estimating local mean signal power level in a Rayleigh fading environment," *IEEE Trans. Veh. Technol.*, pp. 956–959, May 1999.

[23] P. Lancaster and M. Tismenetsky, *The Theory of Matrices*, Second ed. London, U.K.: Academic, 1985.

[24] U. Grenander and G. Szegö, *Toeplitz Forms and Their Applications*. New York: Chelsea, 1984.

[25] R. Gray, "On the asymptotic eigenvalue distribution of Toeplitz matrices," *IEEE Trans. Inform. Theory*, vol. 18, pp. 725–730, Nov. 1972.

[26] W. F. Trench, "Asymptotic distribution of the even and odd spectra of real symmetric Toeplitz matrices," *Linear Algebra and Its Applications*, pp. 155–162, 1999.

[27] K. Yao, R. Hudson, C. Reed, D. Chen, and F. Lorenzelli, "Blind beamforming on a randomly distributed sensor array system," *IEEE J. Select. Areas Commun.*, pp. 1555–1567, Oct. 1998.

[28] P. Voois, "A theorem of the asymptotic eigenvalue distribution of Toeplitz-block-Toeplitz matrices," *IEEE Trans. Signal Processing*, vol. 44, pp. 1837–1841, July 1996.

[29] T. Koga and F. Cheng, "Extension of the Toeplitz theorem and its application," in *Proc. GLOBECOM*, vol. 1, 1987, pp. 263–267.

[30] R. Durrett, *Probability: Theory and Examples*, Second ed. New York: Duxbury, 1996.

[31] I. Gelfand and S. Fomin, *Calculus of Variations*. Englewood Cliffs, NJ: Prentice-Hall, 1963.

[32] D. Hawkins and R. Wixley, "A note on the transformation of chi-squared variables to normality," *Amer. Statistician*, vol. 40, pp. 296–298, Nov. 1986.

[33] R. Narasimhan and D. Cox, "Speed estimation in wireless systems using wavelets," *IEEE Trans. Commun.*, vol. 47, pp. 1357–1364, Sept. 1999.

[34] ——, "Estimation of mobile speed and average received power in wireless systems using best basis methods," in *Proc. 33rd Asilomar Conf. on Signals, Systems, and Computers*, Pacific Grove, CA, 1999, pp. 300–305.

[35] S. W. Kim and A. Goldsmith, "Truncated power control in CDMA communications," in *Proc. IEEE GLOBECOM*, 1997, pp. 1488–1493.
[36] G. Korn and T. Korn, *Mathematical Handbook for Scientists and Engineers*. New York: McGraw-Hill, 1961.

Shuangqing Wei (S'99) received the B.E. and M.S. degrees in electrical engineering from Tsinghua University, Beijing, China, in 1995 and 1998, respectively. He is currently working toward the Ph.D. degree in electrical engineering at the University of Massachusetts, Amherst.

His research interests include statistical signal processing, channel coding in wireless communications, and information theory.

Dennis L. Goeckel (S'89–M'92) received the B.S.E.E. degree from Purdue University, West Lafayette, IN, in 1992, and the M.S.E.E. and Ph.D. degrees, both in electrical engineering, from the University of Michigan, Ann Arbor, in 1993 and 1996, respectively.

From 1987 to 1992, he worked at Sundstrand Corporation. From 1992 to 1996, he was a National Science Foundation Graduate Fellow at the University of Michigan. In September 1996, he joined the Electrical and Computer Engineering Department, University of Massachusetts, Amherst, where he is currently an Associate Professor. His research interests are in the design of digital communication systems, particularly for wireless communications applications.

Dr. Goeckel is the recipient of a 1999 CAREER Award from the National Science Foundation. He is an Editor for the IEEE TRANSACTIONS ON WIRELESS COMMUNICATIONS.